The Influence of Defects on the Short-term Breakdown Characteristics and Long-term dc Performance of LDPE Insulation

G. Chen and A. E. Davies
Department of Electrical Engineering
University of Southampton, UK

ABSTRACT

Extruded polyethylene is used as the bulk insulation for ac HV cables because of its high electric resistivity and breakdown strength. Although the material at present has limited use in dc power cables, it is used extensively in submarine optical communication cable systems. This paper reports on the study of the short-term characteristics and long-term performance of low-density polyethylene (LDPE) insulation under dc electric stress. The results are presented in which controlled defects as found in practical systems (voids, metallic and non-metallic particles) were introduced into well characterized polymer material so that their influence on electrical strength and breakdown mechanisms could be determined. Samples were compression-molded under laboratory conditions and subjected to ramp-to-failure and electrical aging tests at various stresses. Weibull statistics are used to analyze the results. Examination of electrically aged samples indicates an oxidation degradation around the defects due to stress enhancement. From the failed samples a value of n in the inverse power model was estimated. The residual life of aged samples also was examined.

1 INTRODUCTION

CONSIDERABLE effort has been made to improve the electrical performance of solid polymeric insulation systems. However, there is also considerable evidence [1] that defects in the material can cause premature electrical failure. Generally, there are four kinds of defects; voids, inclusions (metallic and non-metallic), protrusions from semiconducting layers and inhomogeneities (crystalline scale). Both electrical and water trees can be initiated at these defects, leading to premature failure.

A number of experimental investigations [2, 3] have shown that the lifetime of polyethylene (PE) insulated cables can be reduced due to the inclusions. Coppard *et al.* [4] investigated the effect of irregular aluminum particles on the dielectric breakdown of PE and showed that ac electric breakdown stress decreases rapidly with an increase in particle concentration. The results were explained based on the bond percolation model developed by Duxbury *et al.* [5]. However, defects are found to be singular and randomly distributed in the material. Work carried out by Hagen and Ildstad [6, 7] showed that the addition of conducting iron and copper particles reduced the short term ac breakdown stress of the material from 107 kV/mm to 70 and 35 kV/mm for spherically and irregularly shaped particles, respectively. For glass particles the breakdown stress was reduced to 55 kV/mm, regardless of the shape of the particles.

It is well known that the dielectric strength of PE decreases with prolonged exposure to electric stress. During this aging process localized electric breakdown occurs, resulting in the formation of microscopic channels. It is the growth of these that eventually causes the insulation to fail [8]. Although the operating stresses are well below the measured short-term electric breakdown strength of the polymer, electrical breakdown occurs in service with failure times ranging from hours to years [9]. A significant number of these failures are initiated by inherent defects. Improvements in manufacturing techniques and quality control have led to a significant reduction in void size and levels of contamination. However, economic and practical considerations mean that internal defects cannot be completely eliminated. On the other hand there is a growing economic pressure to extend the life of electrical apparatus by operating at increased stress levels. In order to achieve a significant increase in operating electric stresses and service life of cables, the influence of defects on the mechanisms responsible for initiation and aging of the insulation needs to be understood and defined.

A considerable amount of work has been carried out on the influence of the defects on the ac performance of PE, yet very limited studies have been carried out under dc conditions. In this paper, we report the results of an investigation in which a variety of controlled defects were deliberately introduced into well characterized polymer systems, so that their influence on electric strength and breakdown mechanism under dc voltage could be determined. The defects include metallic (aluminum and bronze), non-metallic (glass beads and amber) and voids. Samples

1070–9878/0/ $3.00

Table 1. Characteristics of LDPE. X_{SB} short-chain branching, largely ethyl and butyl; X_{LB} degree of long-chain branching.

Characteristic	Range	Unit
M_n	1.4- >1.9×10^4	
M_w	1.8- >2.7×10^5	
X_{SB}	20 - >25	CH_3 / 1000 C atoms
X_{LB}	2.5- >4.0×10^{-4}	
density	0.922- >0.924	g/cm^3
crystallinity	47.4	%
melting point	110	°C

were compression-molded under laboratory conditions and subjected to constant ramp dc voltage until failure. Weibull statistics are used to analyze the results. Life tests have been carried out at three different stress levels with the aim of determining both the life exponent n in the inverse power model $tE^n = k$, and the effect of defects on the life of the insulation.

Optical microscopy and Fourier transform infrared (FTIR) were used to examine the electrically aged samples. Based on the results from both short-term breakdown and long-term aging, a value of n in the power model was estimated. The residual life of aged samples was also examined.

2 EXPERIMENTATION

The LDPE used, Unifos HFDS 4201, supplied by Unifos Kemi AB Sweden, has the characteristics as given in Table 1.

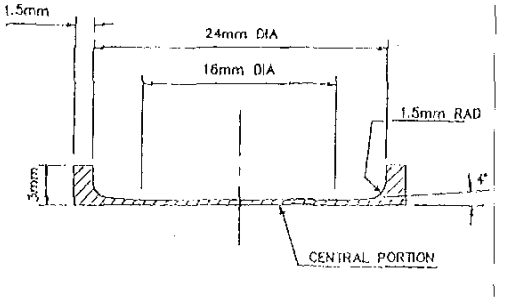

Figure 1. A schematic diagram of the sample.

The samples were manufactured using a pressure molding process. Prior to the molding of the sample the as-received granules were pressed between heated plates to produce plaques of ~ 0.5 mm thickness. From these sheets, circular blanks were produced. Two blanks were placed into the mold (*i.e.* die, curved electrode and flat electrode), heated to 150°C under a pressure of 160 kN/cm^2 and then quench cooled to room temperature. A schematic diagram of the sample is shown in Figure 1. The disc-like samples had a Rogowski profile in order to minimize edge breakdown effects.

For samples with conducting defects, the particles were placed between two LDPE blanks and the sample manufactured using the method described above. The defects were located and their positions recorded after sample manufacture, so that the failure sites after testing could be compared with known particle positions. In general, three to four particles were evenly distributed in the central region of each sample.

The samples containing glass beads as non-conducting particles were fabricated in a way similar to those containing conducting particles.

The as-received LDPE granules used in the present work was found to contain yellowish or brown particles called 'amber'. The ambers surrounded by a matrix of PE were removed from thin films prepared by pressing the granules between two heated glass plates. They usually were found to be irregularly shaped particles and appeared very clear with distinct edges. Selected ambers were then placed in position between two circular blanks of LDPE and samples manufactured in the same way as described above.

For a controlled experiment, voids should be of spherical shape and of a particular size. A number of methods to produce voids had been tried *e.g.* blowing agents, micro-injection of liquids and the three layer method, but were all found to be unsuccessful. However, some success was achieved producing a capillary void. A thin metal filament wire of 50 or 100 μm under tension was placed across the mold, LDPE granules were placed in the mold and pressure molded at 150°C into samples. When cooled, the wire was withdrawn leaving a capillary void in the LDPE samples. The disadvantage with this method is that a cylindrical void is formed rather than a spherical one. The thickness of the sample was ~250 μm with capillary voids of 50 and 100 μm.

Aluminum electrodes with a diameter of 19 mm were evaporated onto both sides of the samples. The short-term dc electrical breakdown tests were carried out with the samples immersed in silicone oil to prevent flashover.

When the samples containing capillary voids were tested, both ends of the capillary were sealed, so that the gas inside the void was maintained. The voltage rise rate was kept constant at 60 kV/min.

Traditionally, the inverse power law [10] has been used to estimate the expected service life of electrical insulation. This empirical relationship has been shown to be applicable in limited solid and liquid impregnated systems at high electric stress levels. Based on this model, the n value can be determined by carrying out several tests of the time to failure at different constant stresses. These accelerated aging tests can be performed with high stress levels and the life under service conditions obtained by extrapolation of the results from the plot of $\log E$ *vs.* $\log t_F$. In the ac case, the highest stress may be set just below the partial discharge (PD) inception stress E_i. In the dc case, PD activity is random, and E_i difficult to define. Therefore, a maximum stress of ~1/5 of the material's short-term breakdown stress was chosen as the highest stress for the aging tests. Three voltage levels were chosen at 12, 6 and 3 kV, corresponding to an average stress 100, 50 and 25 kV/mm for control samples; 75, 37.5 and 18.75 kV/mm for the samples containing metallic inclusions; and 40, 20 and 10 kV/mm for the samples containing a capillary void. All the stresses are significantly higher than the service stress (~1.6 kV/mm) employed in repeater fiber optical telecommunication submarine cable systems.

In the case of long-term aging tests, in order to achieve the required stress, the sample thickness differed slightly from that used for short-term breakdown measurements. They were 120 μm for control samples, 160 μm for the samples containing metallic inclusion and 300 μm for the samples containing a capillary void. Again, aluminum electrodes were evaporated to both sides of the sample. The samples were subjected to the stresses given above and the times of failure were recorded.

3 EXPERIMENTAL RESULTS AND DISCUSSION

3.1 SHORT-TERM CHARACTERISTICS

When assessing the test results for the breakdown of polymeric insulation, the use of a statistical method is often required. Weibull distribution [11] is now widely accepted which is based on the fact that the failure of the whole system depends on the failure of the weakest point in the system. The probability of the failure takes the form of

$$P(E) = 1 - \exp\left[-\left(\frac{E}{\alpha}\right)^{\beta}\right] \quad (1)$$

where α is the scale parameter and represents the electric stress (characteristic stress) for which the failure probability is 0.632, β is the shape parameter which is a measure of the spread of breakdown stresses.

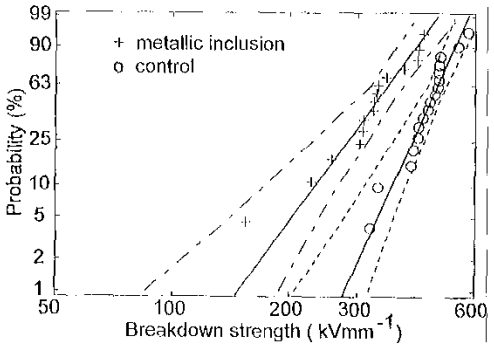

Figure 2. Weibull plot of samples containing 55 to 65 μm bronze particles.

Figure 2 shows the Weibull plot of the breakdown stress of the samples containing bronze particles with a nominal size from 55 to 65 μm. The results with control samples are also presented. The 90% confidence bounds do not overlap, indicating that the two sets of data differ significantly. The characteristic stresses obtained are 480 kV/mm for control samples and 358 kV/mm for samples containing bronze particles respectively.

The effect of different conducting particles on the electrical performance of the material was achieved by coating glass beads with aluminum. Similar characteristic breakdown stress (340 kV/mm) was obtained with samples containing glass beads (~60 μm in diameter) with evaporated aluminum coating.

Glass beads also were embedded into LDPE as a non-metallic inclusion. Figure 3 shows the Weibull plot of the breakdown data. Surprisingly, the characteristic stress was 374 kV/mm, only slightly higher than the value obtained from aluminum coated glass beads. It differs significantly from the control samples.

Examination under an optical microscope indicated that the breakdown sites in all tested samples were at the inclusions.

A typical infrared (IR) spectrum obtained from micro-FTIR for an amber defect is shown in Figure 4. The obvious differences between LDPE and the amber are the two absorption peaks from OH groups and CO groups. The population of amber particles in the LDPE is reported

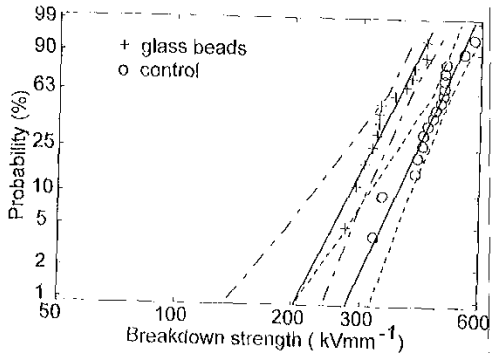

Figure 3. Weibull plot of samples containing ~60 μm glass beads.

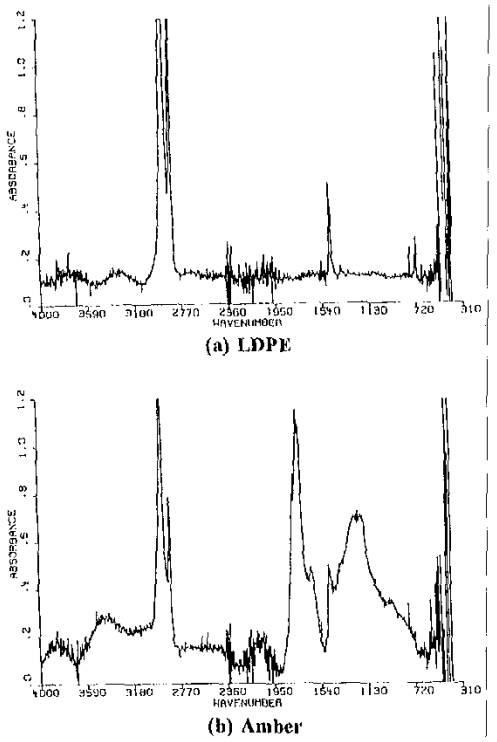

Figure 4. Micro-FTIR spectra of LDPE and amber. (a) LDPE, (b) amber.

as high as 40000/kg [12]. They were considered to be formed during the original extrusion process in the production of the granules and range in size between 10 and 30 μm and have various shapes. There was no major difference in the electrical breakdown strength between the control samples and the samples containing ambers. None of the failure sites were at the amber defects.

Figure 5 shows the Weibull plot of breakdown data from samples containing 100 and 50 μm capillary voids. The characteristic breakdown stresses were 136 and 183 kV/mm for 100 and 50 μm diameter voids, respectively.

Compared with the control samples it is noted that the introduction of the voids reduced the characteristic breakdown stress significantly. The results obtained from different samples are summarized in Table 2.

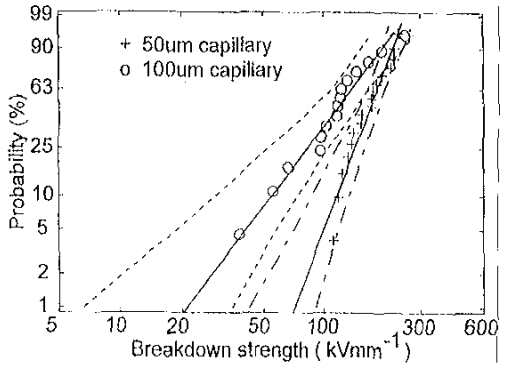

Figure 5. Weibull plot of samples containing 50 and 100 μm capillary voids.

Table 2. Characteristic breakdown strength for samples.

Inclusion type	E_b kV/mm <90%	α	>90%	β
LDPE	453	480	505	8.4
coated Al	310	340	369	6.3
glass beads	348	374	399	7.6
bronze	323	358	392	5.2
ambers	446	471	495	8.3
100μm void	110	137	165	2.5
50μm void	166	183	200	4.8

The shape parameter β in the Weibull distribution represents a spread of test data: the higher the β, the narrower the data distribution. It is known generally that breakdown, even in the control samples, is determined by the defects. When the artificial inclusions are a contributing factor, the shape parameter will be decided by the distribution and the size of the inclusions. Lower values of β in the samples containing voids may be associated with the scattering of PD inception within the voids.

Similar to ac stressing, the characteristic breakdown stress does not change significantly with different conducting particles (assuming the size is similar). It has shown in the percolation model [13] that a single conducting defect will reduce $E_c(o)$ to $\frac{1}{4}pE_c(o)$ (where p is the volume fraction of the particle). Because the inclusions were isolated, in the present case for an individual defect its effect on breakdown can be considered as contribution from a single defect. If we assume $E_c(o)$ is a value taken for control samples, then $\frac{1}{4}pE_c(o) = 377$ kV/mm, which is similar to that obtained from the samples containing conducting particles.

In the case of the sample containing glass beads, under ac conditions, the stress distribution is determined by the permittivities of the materials. The permittivity of the glass is $\sim$8, while the permittivity of conducting particles tends to be infinite. This causes a significant difference when they are embedded into the PE which has a permittivity of $\sim$2.25. The stress enhancement in the sample containing conducting particles is higher than that in the samples containing glass beads. However, the electric stress distribution under dc condition is determined by the conductivities. The conductivity of glass is $\sim 10^{-9}\Omega^{-1}$m^{-1}, while that of the PE is $\sim 10^{-18}\Omega^{-1}$m^{-1}. The conductivity of the glass is much higher than that of superclean LDPE and its effect is not very different from the metallic inclusions. This may explain why the samples containing glass beads show a similar result to the sample containing metallic inclusions.

Another possible reason for lower breakdown stress is the poor adhesion between the inorganic metals or glass and the polymer molecular chains, which may result in small voids at the interface. The work carried out on the same material, but under impulse voltage conditions, demonstrated that the wettability of metallic particles has a significant effect on the breakdown stress [14]

Another factor which could influence the breakdown is the formation of trapped charge due to the non-uniform conductivity [15] and trap sites at the interfaces. This charge can cause localized stress enhancement leading to failure initiation. Common techniques such as the laser induced pressure propagation (LIPP) method [16] and the pulsed electroacoustic (PEA) method [17] would have great difficulty in accurately measuring the space charge on such a small scale ($\sim 100\ \mu$m). A new approach using an acoustic lens [18] may provide an effective tool to measure charge build up at defect boundaries. Work using such a technique to monitor charge trapping is in hand and the results will be reported at a future date.

Although a heavily oxidized LDPE shows a decrease in the dc breakdown stress [19], in the present research the embedded ambers do not appear to affect the dc breakdown stress of LDPE. Samples containing ambers show similar results to the control samples. This indicates that the amber has no major effect on the short-term electrical performance. This may be explained by the fact that ambers are organic and consequently disturb the PE structure far less than inorganic metallic particles. Therefore no microvoids can be formed. Another possible reason is that the size of the ambers under investigation is not large enough to compete with other defects within the material.

For the case of voids, the difference in the breakdown values for 100 and 50 μm capillary voids is obvious. The decrease in β with the introduction of a capillary void is consistent with other inclusions. Also, in the present case the decrease may be associated with the surface damage inside the capillary void caused by the withdrawal of the wire used to form the void.

In the case of capillary voids, the localized breakdown (PD) may start from the void when the stress within the void exceeds the breakdown stress of the air and finally leads to a complete failure of the sample. Because the void generally has a much lower breakdown stress than the LDPE, the breakdown stress of the system is determined by the behavior of the void. In the case of the metallic inclusions, the breakdown may start from the interface between an inclusion and the LDPE towards the electrodes. The results from electric stress computation [20] indicate that an electric stress enhancement occurs at the interfaces. Because the LDPE has a much higher breakdown stress, the breakdown stress of the system may still be quite high compared to samples containing voids. If a small void is developed due to lack of the adhesion between particles and the polymer, the breakdown process may be similar to that occurring in the sample containing a large gas void. However, the PD inception voltage will be much higher than that for the large void, hence giving a higher breakdown stress value.

3.2 LONG-TERM PERFORMANCE

A complete set of breakdown data was obtained for the samples aged at 12 kV, whereas no data were available for samples aged at 3 kV, and an incomplete data set for samples aged at 6 kV. With only a complete single time to failure data set (12 kV), the exponent of the inverse power model cannot be determined. In ac conditions, according to [21], both ramp and constant stress test results can be used to predict the life time of the insulation if the following assumptions and conditions are satisfied,

1. the degradation and failure mechanisms are the same for constant and ramp tests,
2. constant stress tests are performed at the breakdown stress value from the ramp test,
3. the distribution failure probability is the same for constant and ramp tests.

The time to failure t_p of the ramp test can be converted into the time to failure t_c for the constant stress test by

$$\frac{t_p}{n+1} E_p^n = t_c E_c^n = k \tag{2}$$

where k is a constant.

However, in dc conditions the effect of the ramp rate is more complicated due to charge injection and trapping, and Equation (2) may not hold. In the present study, the failure sites both in the ramp and long-term aging (constant stress) tests were all located on the defects which might indicate the same mechanism of failure. In order to construct the life curve from the ramp breakdown and constant stress tests, we have located the characteristic ramp breakdown stress E_c at the time $t_p = E_c d/R$, where d is the thickness of the sample and R is the ramp rate. Compared with the ac case, this procedure overestimates the time to breakdown at stress E_c and underestimates the life exponent n, leading to a pessimistic extrapolation to low stresses.

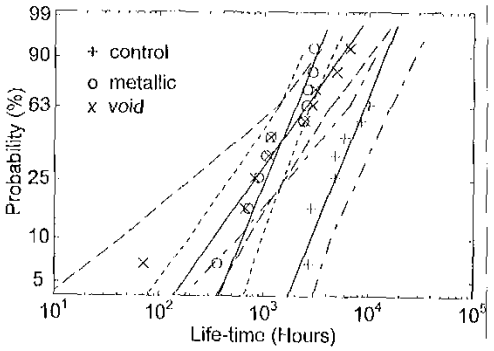

Figure 6. Weibull plots of different samples aged at 12 kV.

Figure 6 shows the Weibull plot for control samples, the samples containing 50 to 60 μm metallic inclusions and the samples containing a 50 μm capillary void, aged at 12 kV. The characteristic times to failure are 9018, 1974 and 2454 h, respectively. The time exponents in Weibull distribution are all above unity as shown in Table 3, indicating a progressive deterioration of the material [11]. The life curves for the samples containing defects are shown in Figure 7 and the life exponent n values and constants are given in Table 3.

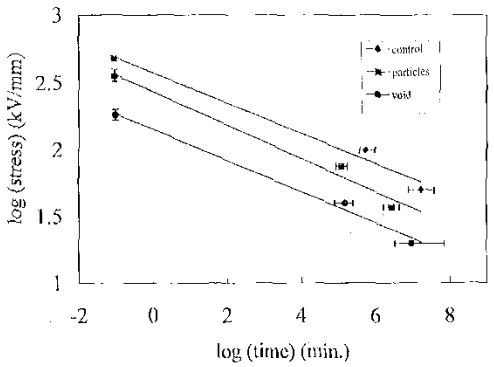

Figure 7. Life curves for different samples. The bars to each line in this plot are 90% confidence limits and not error levels.

Table 3. n value for various defects.

Sample	Control	Metallic	50μm void	Unit
E_p	480	358	183	kV/mm
t_p	0.960	0.955	0.915	min
E_c	100	75	40	kV/mm
t_c	9018	1974	2454	h
β	1.92	1.92	1.11	
n	9.97	8.97	9.42	
k	7.85×10^{23}	1.30×10^{20}	3.03×10^{18}	kV/mm h

Data from the samples stressed at a voltage of 6 kV were also estimated based on the same principle described above. The samples that survived the aging test were ramped to failure and equivalent times t_c were calculated from Equation (2). The total time was taken as the sum of the aged time and t_c. The results obtained for the three sets of samples aged at 6 kV were included with the ramped to failure and the aged samples at 12 kV results as shown in Figure 7. The characteristic times obtained fit the inverse power law reasonably well.

The two constants n and k in the inverse power model are related to the material. Initially, it was thought that the introduction of the defects into the polymer may reduce the n value. However, the n values in Table 3 show little change with different defects, but the k value does vary in the following order: k_c (control) $>k_m$ (metallic) $>k_v$ (void). Thus this value also is important for determining the life time of the material. Similar to the short-term characteristics, the life time of the LDPE insulation is reduced by the introduction of the defects into the material. Capillary voids are found to be more detrimental to the insulation than metallic inclusions of similar size.

As mentioned previously, poor adhesion between metallic inclusion and polymer may occur, with small voids being formed between the inclusions and the polymer material. During the electrical aging process, degradation is likely to occur. In the case of control samples, it has been reported [22] that aging a sample above a critical field under ac, submicrocavities can be formed. This condition may occur under dc as the movement of space charge can generate an oscillating field [23]. If the voids are responsible for failure, it can be assumed that the mechanism of failure is the same for each case, and then similar n values may be reasonable.

Remanent life breakdown tests for the samples aged at 3 kV also were performed. The characteristic breakdown stresses and β values

Table 4. Residual stress of the samples aged for 2.5 yr.

Sample	E_c, kV/mm		β	
	before	after	before	after
control	480	460	8.4	9.7
metallic inclusions	358	371	5.2	7.6
voids 50μm	183	198	4.8	5.6

are summarized in Table 4. By comparing the 'characteristic stress' values before and after aging, it can be seen that the samples aged at a voltage of 3 kV for 2.5 yr has no major effect on the material, even if it contains small defects. It has been suggested [24] that lifelines should have a stress threshold appropriate to the material, and it is possible that the results from the remanent life breakdown tests do indicate a threshold stress. Although it is difficulty to pinpoint the exact values of the threshold stress for the samples tested, it is fair to say that the threshold stress is >25 kV/mm for control samples, 18.75 kV/mm for the samples containing metallic inclusion, and 10 kV/mm for the samples containing voids.

4 SAMPLE CHARACTERIZATION AFTER AGING

In order to obtain information regarding possible aging mechanisms, optical microscopy and IR spectroscopy also were carried out on the material around the defect area.

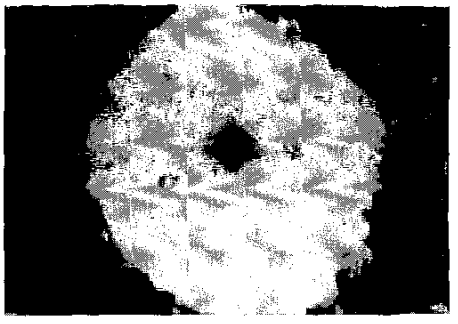

Figure 8. A failure site in a sample containing metallic inclusions where oxidation has been developed (mag. 70×).

The samples were cleaned with methanol to remove the aluminum electrodes and then dried. All failure sites were located on the metallic particles in the polymer. Because of the power dissipated during the failure of the samples, excessive damage occurred at the breakdown site, making it difficult to determine the failure cause. However, in some instances it was possible to limit the damage. Figure 8 illustrates a failure site where oxidation occurred; the aluminum electrodes around the inclusion were removed due to the local heat generated. Around the failure site the material was yellow in color but differed from that of 'ambers'. No distinct edge can be found as in ambers, and the color changed gradually from dark brown in the center to that of the normal PE color. In addition, multi-failure sites were observed and partial damage was also found in several samples.

The failure sites again were located on the capillary void in all cases. Multi-failure sites were observed also. It is noticed that the capillary void near the failure site had been damaged, presumably due to PD before the failure.

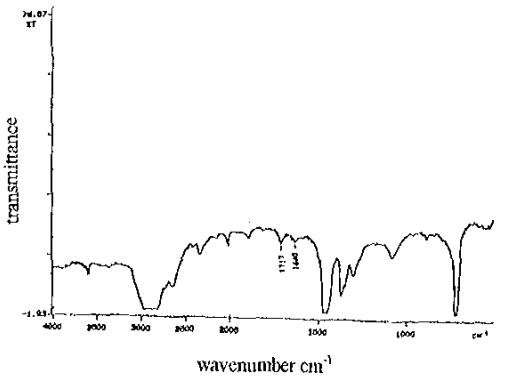

Figure 9. IR spectrum of the area shown in Figure 8 (aged at 6 kV for 2350 h).

IR spectroscopy has been used extensively in polymer degradation research as a tool for examining structure changes and identifying the functional groups present. Figure 9 shows an IR spectrum of the sample containing metallic particles. The area examined around the inclusion is the same as that shown in Figure 8. The absorption at the 1717 cm^{-1} band is quite obvious and indicates oxidative degradation (C=O) in the material. The peak at the 1640 cm^{-1} band is the indication of C=C double bond. As mentioned in the previous Section, a tiny void can be developed due to the adhesion, even during the aging process. As a consequence PD can occur, which will lead eventually to a degradation and failure of the material.

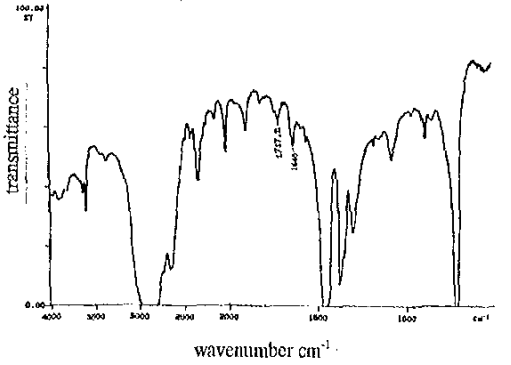

Figure 10. IR spectrum of a sample containing voids (aged at 6 kV for 8364 h).

Figure 10 shows the IR spectra of the sample containing a 50 μm capillary void after aging. It can be seen that oxidation had occurred after 8364 h aged at 6 kV. Apart from the absorption peak at the 1717 cm^{-1} band, a strong absorption peak at 1640 cm^{-1} appeared, which indicates the existence of C=C double bonds. The cause of the oxidative degradation may be due to PD where high energy ions bombard the internal surface. In the presence of oxygen, the material will decompose through chemical reactions.

The change in IR spectrum of the aged control sample also was monitored. Unlike the samples containing defects where extra peaks introduced by electrical stress are obvious, only small peaks appeared in the control sample, presumably due to the lack of severe stress enhancement.

Comparing to thermo-oxidative degradation, a distinct feature for the electrically aged sample is the formation of C=C double bonds, appearing at 1640 cm^{-1} in the IR spectra. No such peak can be found in the case of the thermo-oxidative degradation [19].

IR spectra from the samples aged at 3 kV were obtained also. There is no sign of any chemical change. This is in agreement with the electrical performance.

5 CONCLUSIONS

THE influence of various controlled defects on the short-term dc breakdown characteristics of LDPE have been examined. The metallic inclusions reduce the effective thickness of the samples and cause electric stress distortion resulting in a lower breakdown voltage. The larger the inclusion, the lower the breakdown voltage. Defects with <15 μm diameter have little effect on the electrical breakdown strength of the material.

Unlike under ac stress, glass beads have a similar effect as metallic inclusions under dc conditions, the breakdown stress is reduced significantly.

For a sample containing particles of ~ 60 μm diameter, the characteristic breakdown stress is reduced from 480 kV/mm (for control samples) to ~ 350 kV/mm.

Under dc conditions, ambers have no major effect on the short-term performance. Long-term performance requires further investigation.

Capillary voids are found to be more detrimental to the insulation than metallic inclusions of similar size.

From the electrical aging tests the exponent of the inverse power model for LDPE was found. The following n values have been obtained:

1. $n = 9.97$ for control samples,
2. $n = 8.97$ for the samples containing 55 to 65 μm metallic inclusions,
3. $n = 9.42$ for the samples containing 50 μm capillary voids.

The life time of the LDPE insulation is shortened by the introduction of the defects. Capillary voids, as expected, are found to be more detrimental to the insulation than metallic inclusions of similar size.

Remanent life measurement for the samples aged at 3 kV indicates that there may be a threshold stress for the lifelines.

Optical microscopy has been used to observe the failure sites in electrically aged samples. Several features have been found. All the failure sites were located on the introduced inclusions (metallic particles and capillary voids). In some cases multi-failure sites and partial damage was evident because of several embedded inclusions. The damage inside the capillary voids is caused by PD activity.

The chemical changes caused by electrical aging were assessed using IR spectroscopy. It has been found that the oxidative degradation developed generally was confined to around the inclusions, presumably due to stress enhancement leading to PD in a tiny void. In the case of capillary voids, oxidation may be introduced by PD. The control sample only showed very light oxidation.

Compared to thermo-oxidative degradation, a distinct feature in the present case is the formation of C=C double bonds at 1640 cm^{-1}, caused by electrical stressing of the material.

REFERENCES

[1] J. D. Mintz, "Failure analysis of polymeric-insulated power cable", IEEE Trans Power Appr. Syst. Vol. 103, No. 12, pp. 3448-3453, 1984.

[2] P. H. F. Morshuis, F. H. Kreuger and P. P. Leufkens, "The effect of different types of inclusions on PE cable life", IEEE Elec. Insul. Vol. 23, pp. 1051-1055, 1988.

[3] W. Weibenberg, W. Mosch and M. Eberhardt, "Breakdown voltage of PE/XLPE insulated cables with included imperfections", 5th ISH, Paper No. 23.25, 1987.

[4] R. W. Coppard, J. Bowman, L. A. Dissado, S. M. Rowland and R. T. Rakowski, "The effect of aluminum inclusions on the dielectric breakdown of polyethylene", J Phys. D: Appl. Phys. Vol. 23, pp. 1554-1561, 1990.

[5] P. M. Duxbury, P. D. Beale and P. L. Leath, "Size effects of electrical breakdown in quenched random media", Phys. Rev. Lett. Vol. 57, pp. 1052-1055, 1986.

[6] S. T. Hagen and E. Ildstad, "Reduction of AC-breakdown strength due to particles in XLPE cable insulation", Conf. on Power cables and Accessories 10 kV-500 kV, pp. 165-168, 1993.

[7] S. T. Hagen and E. Ildstad, "The effect of inclusions on ac breakdown of XLPE cable insulation", CEIDP, pp. 367-373, 1991.

[8] R. M. Eichhorn and in, *Engineering Dielectrics*, Vol. IIA, Bartnikas and Eichhorn eds. ASTM Technical Publications 783, 1983.

[9] K. D. Kiss, H. C. Deepken, N. Srinivas and B. S. Bernstein, "Aging of Polyolefin Insulation", in *Durability of macromolecular materials*, Vol. 95, Ed. by R. K. Eby (ACS Symp. Ser.,) pp. 433-466, 1979.

[10] L. A. Dissado, I. Doble, S. V. Wolfe, A. E. Davies and G. Chen, "Electrical reliability of dc operated submarine telecommunication cables", IEEE Trans. Dielectrics and Elect. Insul., Vol. 4, pp. 1–9, 1997.

[11] L. A. Dissado and J. C. Fothergill, *Electrical Degradation and Breakdown in Polymers*, Peter Peregrinus Ltd, London, 1992.

[12] T. Nensi, A. E. Davies, S. Swingler and J. Cooper, "Characterisation of amber defects in polyethylene insulation", IEE 6th Intl. Conf. on DMMA, pp. 318-321, 1992.

[13] P. D. Beale and P. M. Duxbury, "Theory of dielectric breakdown in metal-loaded dielectrics", Phys. Rev. B, Vol. 37, pp. 2785-2791, 1988.

[14] T. Nensi, A. E. Davies, "Electrical aging and breakdown mechanisms in LDPE insulation", NGC/SERC final report, UK, 1992.

[15] R. Coelho, B. Aladenize and F. Guillaumond, "Charge buildup in lossy dielectrics with induced inhomogeneities", IEEE Trans Dielectrics and Elec. Insul, Vol. 4, pp. 477–486, 1997.

[16] P. Laurenceau, J. Ball, G. Dreyfus, and J. Lewiner, "A novel method for the determination of space charge distribution in dielectric', C. R. Acad. Sci. B, B283, pp. 135–138, 1976.

[17] T. Maeno, T. Futami, H. Kushibe and T. Takada, "Measurement of spatial charge distribution in thick dielectrics using the pulsed electroacoustic method", IEEE Trans. Elec. Insul., Vol. 23, pp. 433-439, 1988.

[18] X. Qin, K. Suzuk, Y. Tanaka and T. Takada, "Three-dimensional space-charge measurement in a dielectric using the acoustic lens and PWP method", J. Phys. D: Appl. Phys. Vol. 32, pp. 157-160, 1999.

[19] G. Chen and A. E. Davies, "Effect of thermo-oxidative aging on the electrical performance of low density polyethylene", ICDS'95 Leicester, England, pp. 651-655, 1995.

[20] A. E. Davies and G. Chen, "Electric stress distribution in polymeric insulation containing defect site and space charge", COMPEL Vol. 11 No. 1, pp. 237-240, 1992.

[21] G. C. Montanari and M. Cacciari, "On the electrical endurance characterisation of insulating materials by constant and progressive stress tests", IEEE Trans. Elec. Insul., Vol. 27, pp. 1000–1008, 1992.

[22] J-L. Paral, J-P. Crine and C. Dang, "Electrical aging of extruded dielectric cables-a physical model", IEEE Trans. Dielectrics and Elec. Insul, Vol. 4, pp. 197-209, 1997.

[23] N. Hozumi, T. Takeda, H. Suzuki and T. Okamoto, "Space charge behavior in XLPE cable insulation under 0.2-1.2 MV/cm dc fields", IEEE Trans. Dielectrics and Elec. Insul, Vol. 5, pp. 82–90, 1998.

[24] G. C. Montanari and L. Simoni, "Aging phenomenology and modeling", IEEE Trans. Elec. Insul., Vol. 28, pp. 755-776, 1993.

Manuscript was received on 5 February 1998, in revised form 18 February 2000.